Computational Study on Nonenzymatic Peptide Bond Cleavage at Asparagine and Aspartic Acid

Saron Catak,[†,‡] Gérald Monard,[*,†] Viktorya Aviyente,[*,‡] and Manuel F. Ruiz-López[†]

Theoretical Chemistry and Biochemistry Group, SRSMC, Nancy-University, CNRS, Boulevard des Aiguillettes, B.P. 239, F-54506 Vandoeuvre-les-Nancy, France, and Department of Chemistry, Bogazici University, 34342 Bebek, Istanbul, Turkey

Received: February 21, 2008; Revised Manuscript Received: June 3, 2008

Nonenzymatic peptide bond cleavage at asparagine (Asn) and glutamine (Gln) residues has been observed during peptide deamidation experiments; cleavage has also been reported at aspartic acid (Asp) and glutamic acid (Glu) residues. Although peptide backbone cleavage at Asn is known to be slower than deamidation, fragmentation products are often observed during peptide deamidation experiments. In this study, mechanisms leading to the cleavage of the carboxyl-side peptide bond of Asn and Asp residues were investigated using computational methods (B3LYP/6-31+G**). Single-point solvent calculations at the B3LYP/6-31++G** level were carried out in water, utilizing the integral equation formalism-polarizable continuum (IEF-PCM) model. Mechanism and energetics of peptide fragmentation at Asn were comparatively analyzed with previous calculations on deamidation of Asn. When deamidation proceeds through direct hydrolysis of the Asn side chain or through cyclic imide formation—via a tautomerization route—it exhibits lower activation barriers than peptide bond cleavage at Asn. The fundamental distinction between the mechanisms leading to deamidation—via a succinimide—and backbone cleavage was found to be the difference in nucleophilic entities involved in the cyclization process (backbone versus side-chain amide nitrogen). If deamidation is prevented by protein three-dimensional structure, cleavage may become a competing pathway. Fragmentation of the peptide backbone at Asp was also computationally studied to understand the likelihood of Asn deamidation preceding backbone cleavage. The activation barrier for backbone cleavage at Asp residues is much lower (approximately 10 kcal/mol) than that at Asn. This suggests that peptide bond cleavage at Asn residues is more likely to take place after it has deamidated into Asp.

Introduction

Asparagine (Asn) and glutamine (Gln), two of the 20 most common natural amino acids, are known to be uniquely unstable under physiological conditions; they spontaneously and nonenzymatically deamidate into aspartic acid (Asp) and glutamic acid (Glu), respectively.[1–3] However, deamidation is not the only possible fate for these two amino acids; nonenzymatic peptide bond cleavage at the carboxyl side of Asn and Gln residues has also been experimentally observed.[4–6] The multitude of products observed is most likely due to the tendency of Asn and Gln to form rings.

Deamidation of Asn at acidic pH is known to occur exclusively through a direct hydrolysis mechanism, whereby the neutral side-chain amide is transformed into a carboxylic acid, forming an Asp residue.[7] However, Asn deamidation at neutral pH has been suggested to take place via a cyclic imide; further experimental [8–14] and computational [15–20] studies have supported this idea. In the succinimide-mediated deamidation mechanism, a nucleophilic attack of the carboxyl-side backbone NH to the Asn side-chain carbonyl occurs, forming a cyclic tetrahedral intermediate (Scheme 1). The cyclization step is then followed by deamination, whereby an ammonia molecule is ejected, to form an even more stable intermediate, the succinimide. Subsequent hydrolysis of the amide bonds on the succinimide ring forms the Asp and iso-Asp products. The rate-determining step of this mechanism has been suggested to be the initial cyclization step,[8,15] in which the backbone amide acts as a nucleophile. However, a recent theoretical study on the deamidation mechanism of a small model peptide has shown that the barrier for the cyclization step is much lower with water assistance and that succinimide hydrolysis is the actual rate-determining step of the overall deamidation reaction,[21] noting that results may vary for different $n + 1$ residues. On the other hand, it was also shown that for the same system deamidation through direct hydrolysis of the Asn side chain at neutral pH is at least as feasible as deamidation through a cyclic imide.[22]

Capasso et al. have studied peptide bond cleavage at Asn.[23,24] At elevated temperatures, only backbone cleavage without deamidation has been observed with Asn—Pro sequences, where succinimide formation cannot occur,[4,25–28] whereas Asn—Ile gave both deamidation and peptide fragmentation products. Cleavage products are formed in most peptide deamidation experiments, but the reaction is usually much slower than deamidation. Asn peptide deamidation half-times range from about 1 to 400 days, and Asn cleavage rates range from about 200 to >10000 days.[14] Cleavage of Asn—Pro is the fastest sequence and, because its backbone nitrogen lacks a proton, Asn—Pro deamidates by slow hydrolysis; hence, cleavage is the principal degradative pathway for Asn—Pro sequences.[4,26]

Peptide bond cleavage at Asp and Glu residues has also been reported in peptides and proteins,[29–32] and the occurrence rate is higher than that for Asn and Gln. The side-chain carboxylic

* Authors to whom correspondence should be addressed: e-mail (V.A.) aviye@boun.edu.tr, (G.M.) gerald.monard@cbt.uhp-nancy.fr.
† Nancy-University.
‡ Bogazici University.

10.1021/jp8015497 CCC: $40.75
Published on Web 08/20/2008

SCHEME 1: Succinimide-Mediated Deamidation Pathway

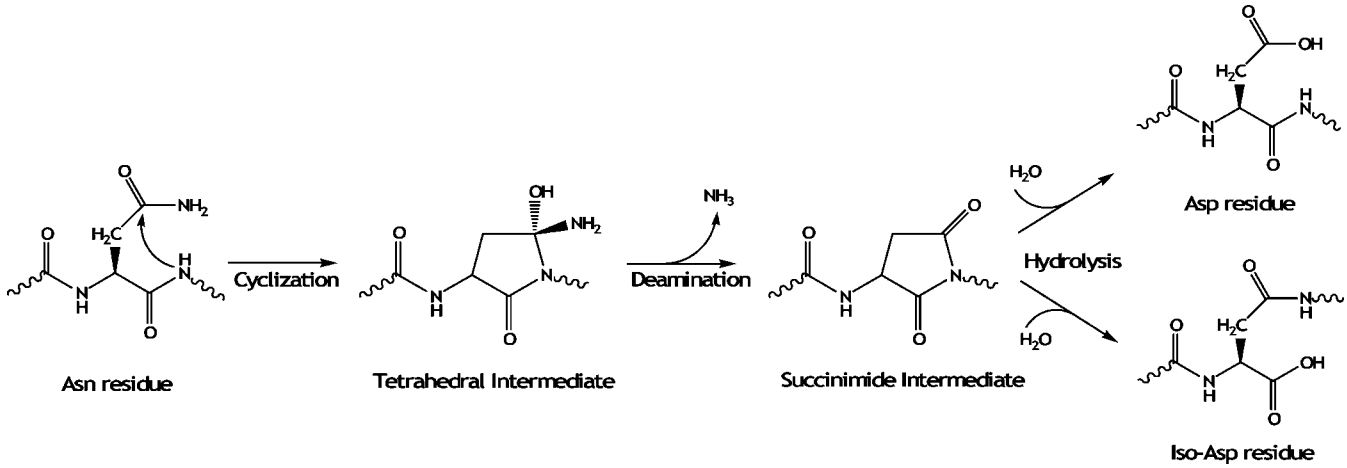

SCHEME 2: Model Peptide with Asn Residue

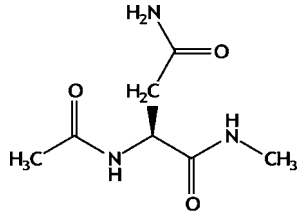

acid group is suggested to play a key role in the cleavage process; this is referred to as the "aspartic acid side-chain effect".[33,34] Because Asn deamidation occurs more readily than backbone cleavage, it is important to investigate the probability of deamidation preceding cleavage, in which case the mechanism and energetics of Asp cleavage become essential.

The aim of this study is to computationally explore the mechanistic differences between deamidation and peptide bond cleavage at Asn and investigate backbone cleavage at Asp. To account for the rate difference between cleavage and deamidation, the energetics of peptide fragmentation will be compared with previous calculations[21] on deamidation of Asn. Moreover, mechanistic and energetic information on Asp backbone cleavage will enable a reasonable prediction for the likelihood of Asn deamidation preceding cleavage. Instead of Asn itself undergoing cleavage, it may convert to Asp via deamidation, and cleavage may take place henceforth. Knowledge on the mechanism and energetics of Asn cleavage may also be useful in cases when deamidation is hindered by protein tertiary structure, in which case cleavage may become a competing reaction.

Computational Methodology

As mentioned earlier, Asn peptide bond cleavage mechanism studied herein will be compared with the Asn deamidation mechanism previously studied by the authors,[21] and therefore the same methodology was employed in this study. Moreover, the same model peptide (Scheme 2) was used for a fair analysis. All structures and energy values reproduced from previous deamidation studies are indicated by an asterisk (*).

Full-geometry optimizations were performed in gas phase—without any constraints—using the density functional theory (DFT)[35–38] at the B3LYP/6-31+G** level.[39–41] The use of this basis set and method in similar peptide systems is well established.[20,21] Stationary points were characterized by a frequency analysis. Zero-point energy and thermal corrections were attained using the ideal gas approximation and standard procedures. Local minima and first-order saddle points were identified by the number of imaginary vibrational frequencies. The species reached by each transition structure was determined by intrinsic reaction coordinate (IRC) calculations.[42,43] Relative free energies of activation ($\Delta G^{\ddagger}$) are calculated as the difference of free energies between transition states and reactants (reactant−water complex when applicable) of each step. Energy values for gas-phase optimizations listed throughout the discussion include thermal free energy corrections at 298 K and 1 atm.

The self-consistent reaction field (SCRF) theory, utilizing the integral equation formalism-polarizable continuum (IEF-PCM) model [44–47] in H_2O ($\epsilon = 78.0$) at the B3LYP/6-31++G** level was used to account for the effect of a polar environment. Bondi radii[48] were used for all solvent calculations using default scaling factors in Gaussian 03.[49] Single-point energies for solvent calculations include nonelectrostatic and thermal free energy corrections obtained from gas-phase optimizations.

Previous computational studies have shown that water molecules have a catalytic effect on deamidation,[21] whereby they serve as efficient proton conduits. The backbone cleavage mechanism was investigated in light of this information. Nomenclature of each optimized transition state structure

SCHEME 3: Side-Chain NH_2 Attack on Asn Backbone Carbonyl To Form a Cyclic Tetrahedral Intermediate

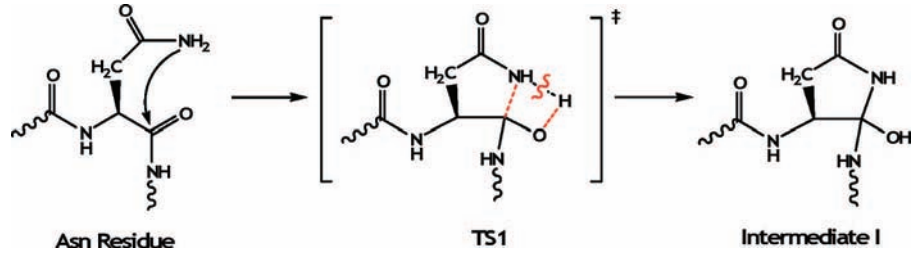

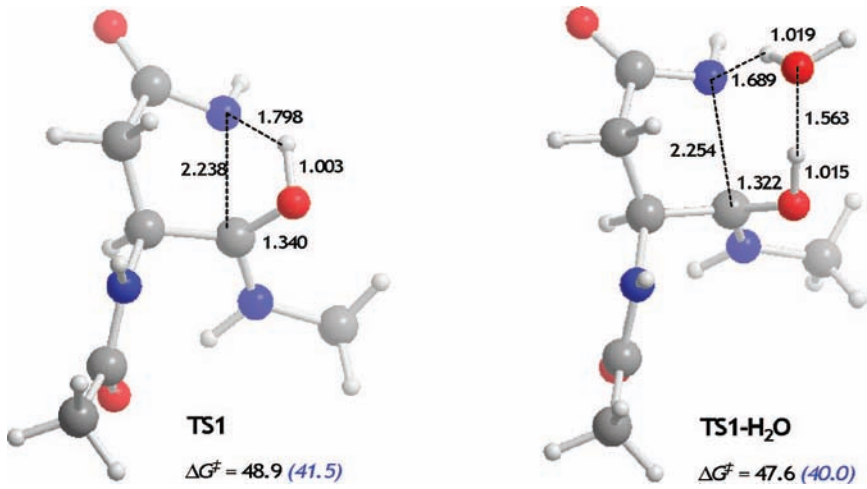

Figure 1. Optimized geometries and free energies of activation for the transition state of side-chain NH_2 attack on backbone Asn carbonyl, concerted nonassisted (TS1) and concerted water-assisted (TS1-H_2O) mechanisms, respectively.

corresponds to the name indicated in the relevant scheme, that is, TSn or TSn-H_2O for water-assisted processes. Comparative discussion of energetics between different mechanisms is always made among species with identical molecularity.

All calculations were carried out using the Gaussian 03 program package.[49] All distances and free energies listed in the discussion are in angstroms (Å) and kilocalories per mole (kcal/mol), respectively. Single-point solvent energies are given in italics.

Results and Discussion

The first part of the discussion elaborates on the mechanism of Asn peptide bond cleavage and comparatively analyzes the mechanism and energetics of peptide fragmentation with deamidation. Alternative fates for intermediates formed during backbone cleavage are discussed in detail. In the second part, backbone cleavage at Asp is investigated and predictions are made on the basis of energetic comparisons.

A. Peptide Fragmentation at Asn Residues. ***1. Cyclization.*** Cleavage of the peptide bond by attack of the Asn side-chain NH_2 is assumed to proceed stepwise, that is, through preliminary attack to Asn backbone carbonyl followed by bond cleavage. Therefore, in the first step, a cyclic intermediate forms (Scheme 3). The side-chain NH_2 group is likely to be more mobile than the backbone NH in a real protein and, therefore, has a better chance of assuming a reactive conformation. The product (intermediate I) of this ring closure is a cyclic tetrahedral intermediate, much like the one that forms in the succinimide-mediated deamidation pathway (Scheme 1).

Both nonassisted and water-assisted mechanisms were modeled for the concerted ring closure via NH_2 attack (Figure 1). The nonassisted attack (TS1) involves the early transfer of a proton from the nucleophile (side-chain NH_2) to the Asn backbone carbonyl's oxygen, as indicated by the rather short O—H distance (1.003 Å) and the elongation in the backbone carbonyl (1.340 Å) compared to the ground-state C=O distance of 1.230 Å. Meanwhile, ring formation is underway (C—N distance = 2.238 Å).

The water-assisted mechanism (TS1-H_2O), in which the proton transfer from the side chain to the backbone goes through a solvent molecule, shows that the H^+ is transferred to the carbonyl group (O—H distance = 1.015 Å) whereas the ring is yet to close (C—N distance = 2.254 Å). The main difference between the concerted waterless (TS1) and water-assisted (TS1-H_2O) transition state is the distance of the breaking N—H bond (1.798 vs 1.689 Å, respectively), which is probably due to the greater flexibility of the latter system.

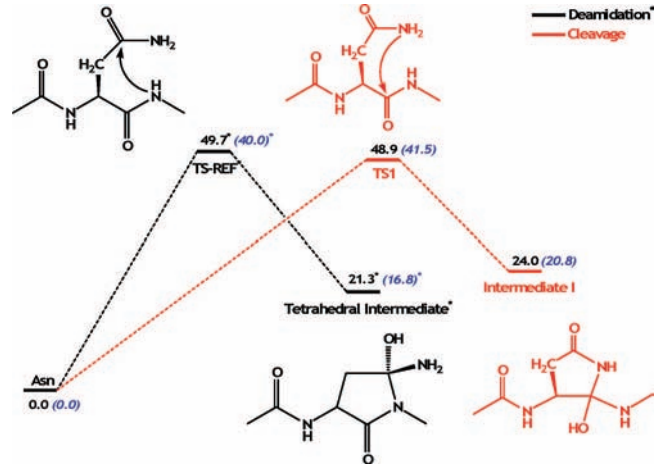

Figure 2. Relative free energies for the concerted nonassisted cyclization step in deamidation[21] and backbone cleavage of Asn.

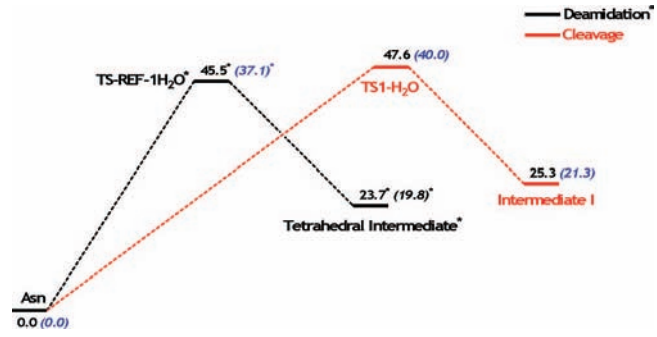

Figure 3. Relative free energies for the concerted water-assisted cyclization in deamidation[21] and backbone cleavage of Asn.

Previous studies on the deamidation mechanism have revealed the catalytic effect of water molecules.[21] In this particular reaction step, the assistance of the water molecule has a favorable effect; however, it is not substantial, as may be seen in the barrier heights reported (Figure 1). Single-point solvent energies in water indicate the stabilizing effect of a polar environment. Both transition states have a somewhat zwitterionic structure and, therefore, benefit from electronic interaction with the dielectric continuum. This is indicated by an approximately

SCHEME 4: Peptide Backbone Cleavage at Intermediate I

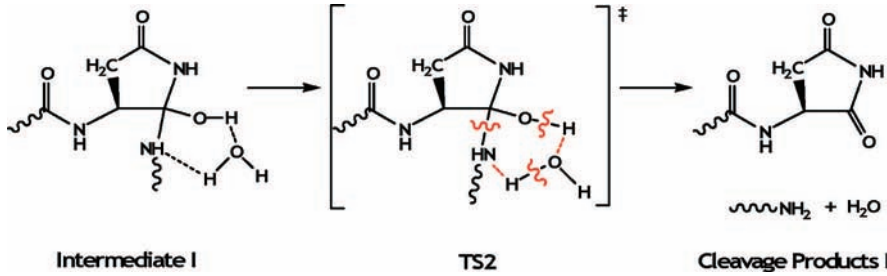

8 kcal/mol decrease in barrier height for both ring closure reactions involving TS1 and TS1-H_2O (Figure 1).

Although the attacking species and the products are different, the free energy of activation for the concerted nonassisted ring closure in deamidation and cleavage pathways is rather close, with <1 kcal/mol free energy difference (Figure 2). Solvent calculations have a similar effect on both mechanisms. The tetrahedral intermediate, formed via the deamidation path, is more stable (by approximately 3 kcal/mol) than the one (intermediate I) formed during cleavage.

The energetics of the water-assisted mechanism for the ring closure steps of cleavage and deamidation are depicted in Figure 3. Water assistance has a more favorable effect on the deamidation cyclization step, lowering the barrier by almost 5 kcal/mol, whereas it causes a decrease of only 1.3 kcal/mol for the cyclization step in the cleavage mechanism. Nevertheless, activation energies for cyclization in both pathways are still comparable.

2. Fates of Intermediate I. Whereas the deamidation pathway (Scheme 1) proceeds with a water-assisted deamination[21] (expulsion of NH_3), intermediate I does not have a free NH_2 group for this to occur. However, it may undergo water-assisted peptide backbone cleavage to form fragmentation products or ring amide hydrolysis to give a noncyclic intermediate. Both reactions are studied below.

a. Peptide Bond Cleavage at Intermediate I. Water molecules assist the fragmentation of the peptide bond on the carboxyl side (Scheme 4) by allowing a proton relay from the −OH on the ring to the carboxyl-side backbone NH group. In this way, the alcohol functionality will be converted into a carbonyl group enhancing conjugation in the cyclic structure, whereas the backbone of the peptide breaks. This will lead to two fragments, one of which bears a free NH_2 group and the other of which will be carrying a succinimide ring at its tail end.

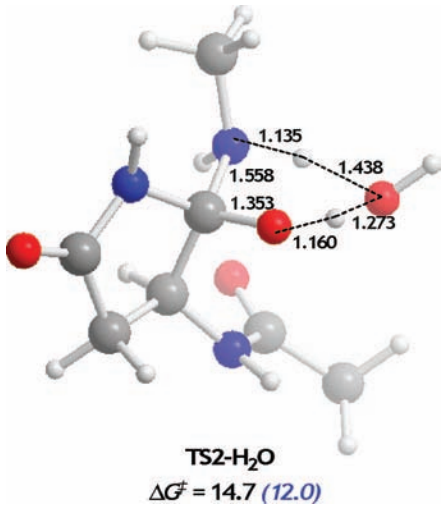

Figure 4. Optimized geometry and free energy of activation for the transition state of cleavage at intermediate I, water-assisted (TS2-H_2O).

Transition state TS2-H_2O shows a slight lengthening in the peptide backbone; the C−N bond distance is in the range of 1.550 Å (Figure 4), quite close to the ground-state bond distance of 1.470 Å, suggesting an early (reactant-like) transition state. The proton transfer is incomplete, as opposed to the case in TS1 and TS1-H_2O (Figure 1). The activation barrier is significantly low (approximately 30 kcal/mol lower) compared to the initial cyclization step (Figures 2 and 3). The assistance of a second water molecule does not have a substantial effect (lowering of 1.3 kcal/mol) on the activation energy for backbone cleavage. This suggests that one water molecule is adequate for modeling the water-assisted reaction.

The transition state geometry for the backbone cleavage step reveals some prerequisites for peptide fragmentation (Figure 4). Considering backbone rigidity in a peptide or protein, the proton transfer from the ring −OH to the backbone NH must take place via a solvent molecule. In addition, proper alignment of these two entities is crucial; the −OH should not be involved in any other intermolecular interactions, the NH group should be in the proper conformation to accept the proton, and, above all, a solvent molecule must form a water bridge between these two entities to facilitate proton transfer. These requirements are not too challenging for a peptide chain with considerable flexibility and access to solvent molecules. However, inside the three-dimensional structure of a protein, the possibility of proper alignment and water bridge availability may be limited.

b. Hydrolysis of the Ring Amide at Intermediate I. Another possible fate for intermediate I is the hydrolysis of the ring amide by nearby water molecules. Hydrolysis can take place via a concerted ring opening (Scheme 5A) or through a gemdiol intermediate (Scheme 5B). Both will give the same product, in which the Asn side chain has been transformed into an Asp.

In the concerted amide hydrolysis reaction, a water molecule attacks the ring carbonyl and the C−N bond breaks, as a proton is transferred from the water molecule to the ring NH. As a result, a carboxylic acid and an NH_2 group emerge (Scheme 5A). In the gemdiol-mediated stepwise mechanism (Scheme 5B), the initial step is the addition of a water molecule to the ring carbonyl, forming a gemdiol intermediate, which consequently undergoes ring opening to reveal the same product (intermediate II).

The water-assisted concerted hydrolysis of the ring amide requires two water molecules (TS3-H_2O) but is assisted by one H_2O only, because one of the water molecules acts as a reactant. As shown in Figure 5, a proton relay occurs—from the water attacking the amide carbonyl to the amide nitrogen—through a water bridge. At the transition state, the proton transfer is incomplete; however, the C−N bond distance (1.578 Å) is substantially lengthened compared to 1.380 Å in the ground

SCHEME 5: (A) Concerted Ring Amide Hydrolysis at Intermediate I; (B) Stepwise Ring Amide Hydrolysis at Intermediate I via a Gemdiol Intermediate

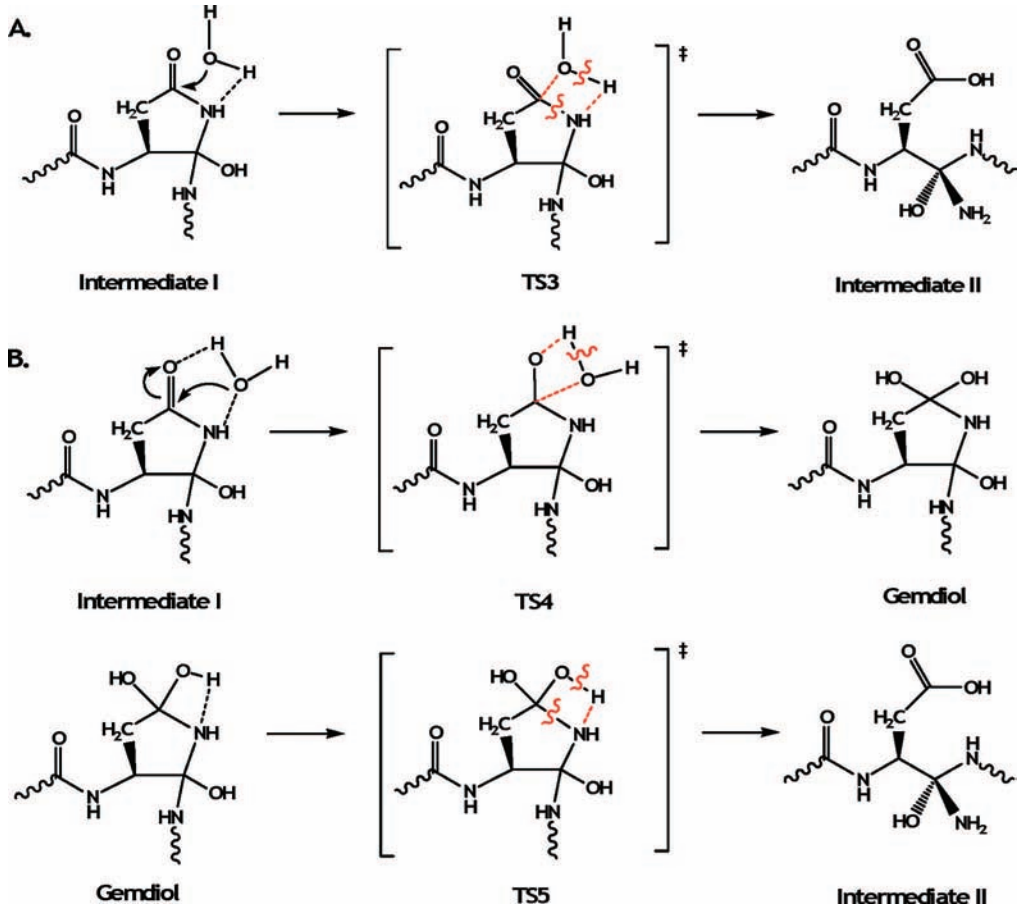

state. In addition, the nucleophilic −OH group is quite close to the carbonyl carbon (C−O distance = 1.814 Å) that it is about to attack.

The first step of the water-assisted gemdiol-mediated mechanism (TS4-H_2O) also involves two water molecules. In this step, the addition of a water molecule to the amide carbonyl occurs. The transition state structure (TS4-H_2O) shows that the proton has been transferred from the water molecule to the amide carbonyl oxygen (O−H distance = 1.018 Å) through a water bridge, with a rather strong hydrogen-bond network (1.530 and 1.581 Å). Incidentally, the C=O double bond is partially broken as indicated by the C−O bond distance of 1.316 Å (1.230 Å in the ground state). The nucleophilic attack distance is 2.104 Å. The cleavage of the ring bearing the gemdiol is depicted in TS5-H_2O (Figure 6). In this step, a proton is transferred from the gemdiol to the adjacent nitrogen via a water molecule. TS5-H_2O may be described as an early transition state (reactant-like), because the proton transfer is not yet complete and ring cleavage is not quite advanced, as indicated by the relatively short C−N bond (1.562 Å compared to the ground-state C−N distance of 1.466 Å).

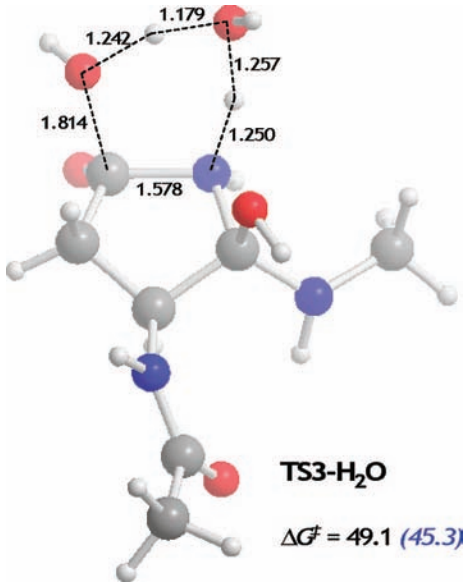

Figure 5. Optimized geometry for the transition state of concerted ring amide hydrolysis, one water-assisted.

Activation energies for the stepwise amide hydrolysis (Figure 7) show that both steps are energetically rather close and the rate-determining step of the two-step process is the ring opening step. Previous studies on amide hydrolysis have suggested that a stepwise mechanism going through a gemdiol intermediate has a considerably lower barrier than a concerted reaction.[50] The energetics of the water-assisted amide hydrolysis modeled herein is in accord with this expectation; the stepwise (gemdiol-mediated) route is more favorable than the concerted pathway by approximately 10 kcal/mol.

The energetic comparison of the possible fates of intermediate I reveals a barrier difference of approximately 25 kcal/mol between carboxyl-side peptide bond cleavage (Figure 4, $\Delta G^{\ddagger}$ = 14.7 kcal/mol) and ring amide hydrolysis (Figure 7, $\Delta G^{\ddagger}$=38.2 kcal/mol). It is apparent that fragmentation is much more favorable than amide hydrolysis at the intermediate I stage.

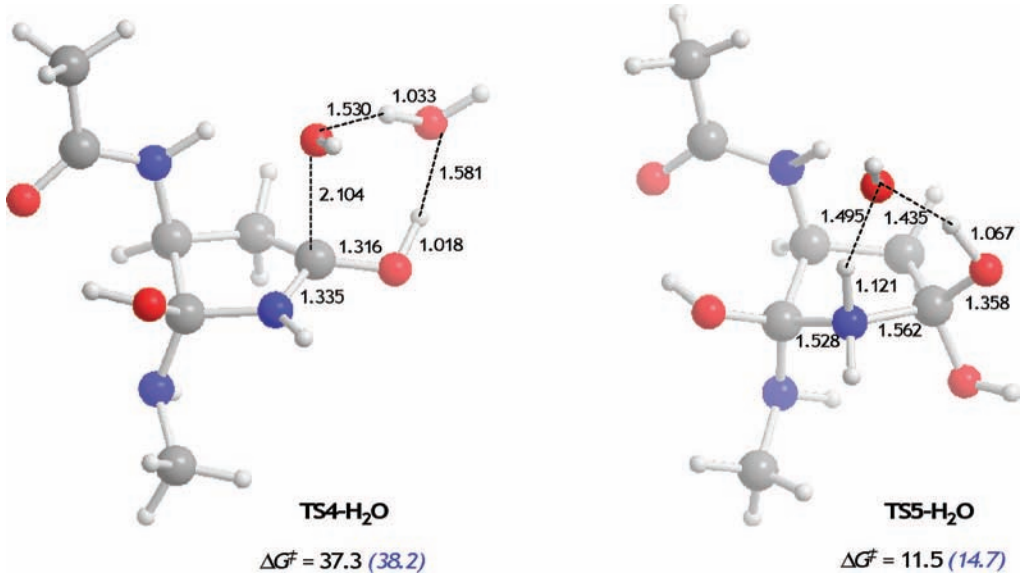

Figure 6. Optimized geometries for the transition states of gemdiol-mediated stepwise ring amide hydrolysis, one water-assisted.

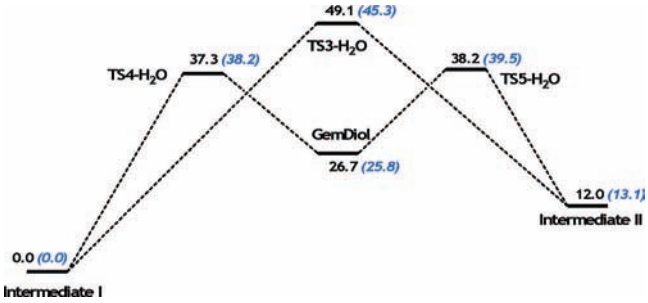

Figure 7. Relative free energies for concerted and gemdiol-mediated ring amide hydrolysis at intermediate I, water-assisted.

However, in some cases, backbone cleavage may be prohibited inside a protein, when the conformational space around the Asn residue is severely restricted by spatial distribution of neighboring residues and/or secondary structure, such as intramolecular H-bonds that form β-sheets or α-helices. In such a case, ring amide hydrolysis may occur at intermediate I to form intermediate II, which can—in a subsequent step—undergo deamination to reveal Asp and/or cleavage at the carboxyl-side peptide bond. This is discussed in the next section.

3. Fates of Intermediate II. Intermediate II may go through a water-assisted deamination step (Scheme 6) that will re-form the backbone peptide bond, and an Asp residue is formed. This route may be suggested as an alternative pathway to the traditional deamidation mechanism (Scheme 1).

Intermediate II may undergo as well peptide backbone fragmentation to reveal cleavage products, given that proper orientation of the backbone is feasible for this reaction (Scheme 7). Cleavage products are similar to those at the intermediate I stage (Scheme 4); however, in this case there are no rings at any of the tail ends. The availability of a water bridge between the backbone NH and −OH group (TS7, Scheme 7) is essential and depends on the position and proper alignment of the backbone NH group.

Relative free energies for deamination and cleavage at the intermediate II stage are shown in Figure 8, together with optimized structures of transition states for these two reactions. The deamination transition state (TS6-H_2O) shows that the ammonia is almost expelled (C−N bond distance = 1.695 Å). In the cleavage case (TS7-H_2O); however, the backbone lengthening has just started (C−N bond distance = 1.583 Å). The cleavage route is energetically favorable by almost 6 kcal/mol.

4. Deamidation versus Peptide Backbone Cleavage at Asn. This study has shown that backbone cleavage at intermediate I is energetically highly favorable and that fragmentation—rather than deamidation—is likely to occur. The overall energetics of peptide bond cleavage at Asn is depicted in Figure 9. The initial cyclization step, with an activation barrier of 47.6 kcal/mol, is incidentally the rate-determining step for peptide bond cleavage at Asn.

Deamidation rates have a large range even for the same primary sequence of amino acids.[51] This suggests that different pathways for deamidation may apply for various conformations of peptides and proteins. In general, it has been assumed that the first step in deamidation consists of a concerted cyclization. We have shown that the corresponding activation barrier is comparable to that found for the equivalent concerted cyclization step in backbone cleavage (either in nonassisted or water-assisted mechanisms, see Figures 2 and 3, respectively). Thus, if deamidation involves concerted cyclization as the first reaction step, deamidation and backbone cleavage would display comparable reaction rates, in contrast with known experimental facts.[14] Actually, we have reported previously that deamidation may proceed through alternative pathways, specifically direct hydrolysis of the Asn side chain[22] or cyclic imide formation via a tautomerization route.[21] Both mechanisms involve lower activation barriers than concerted cyclization provided water assistance is available. Comparison between theoretical and experimental data for deamidation versus backbone cleavage suggests therefore that deamidation proceeds through one of these water-assisted processes.

Note that in case backbone cleavage at intermediate I is inhibited, the hydrolysis of the ring amide may eventually occur, giving rise to an Asp residue (Scheme 5), the major product of the deamidation reaction. However, because intermediate I has only one carbonyl functionality (unlike the succinimide ring), its hydrolysis cannot lead to iso-Asp, a second product often observed in deamidation. Indeed, there are many instances when only Asp is formed as a result of deamidation.[52] Direct hydrolysis of the Asn side chain will also result in Asp formation, exclusively.

SCHEME 6: Deamination (NH_3 Expulsion) at Intermediate II

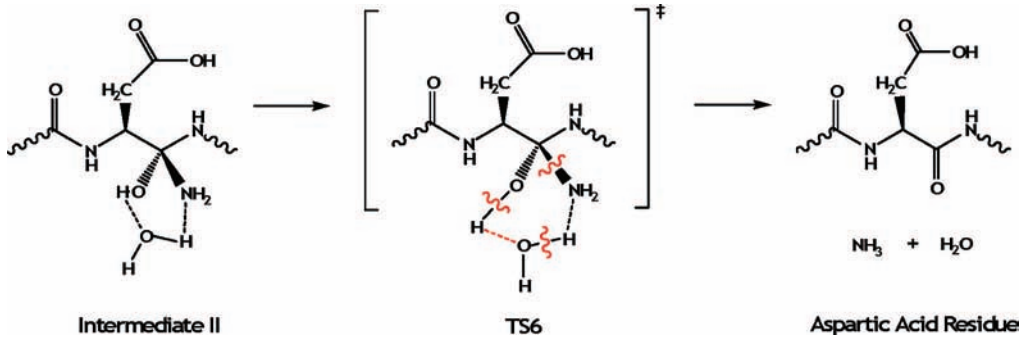

SCHEME 7: Peptide Backbone Cleavage at Intermediate II

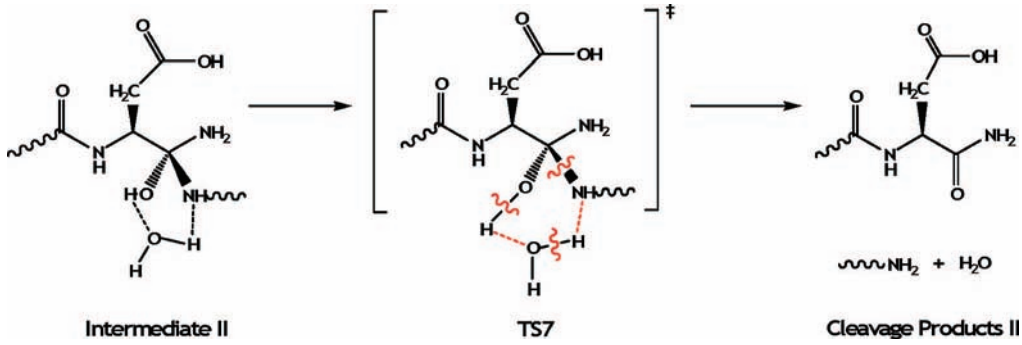

B. Peptide Fragmentation at Asp Residues. Asp can also undergo peptide chain cleavage through formation of an anhydride intermediate and by means of a mechanism similar to peptide bond cleavage at Asn. The Asp side-chain carboxylic acid group is a better candidate for nucleophilic attack than the Asn side-chain NH_2, because the Asp side chain is expected to be present as carboxylate at physiological pH. However, the effective pK_a of the acid may depend substantially on the molecular environment. In the present work, the reaction has been modeled with the carboxylic acid form of Asp rather than the carboxylate anion. The calculated barrier may be considered as an upper limit for the process because the carboxylate anion would be a stronger nucleophile.

The Asp side chain attacks the backbone carbonyl, and a cyclic tetrahedral intermediate (Asp-intermediate I) forms in the initial step (Scheme 8), much like the case in Asn (Scheme 3). The ring closure step is followed by the actual cleavage step (Scheme 8). Cleavage products are similar to those for Asn, except an anhydride ring forms at one of the peptide tail ends, instead of a succinimide ring (Scheme 4).

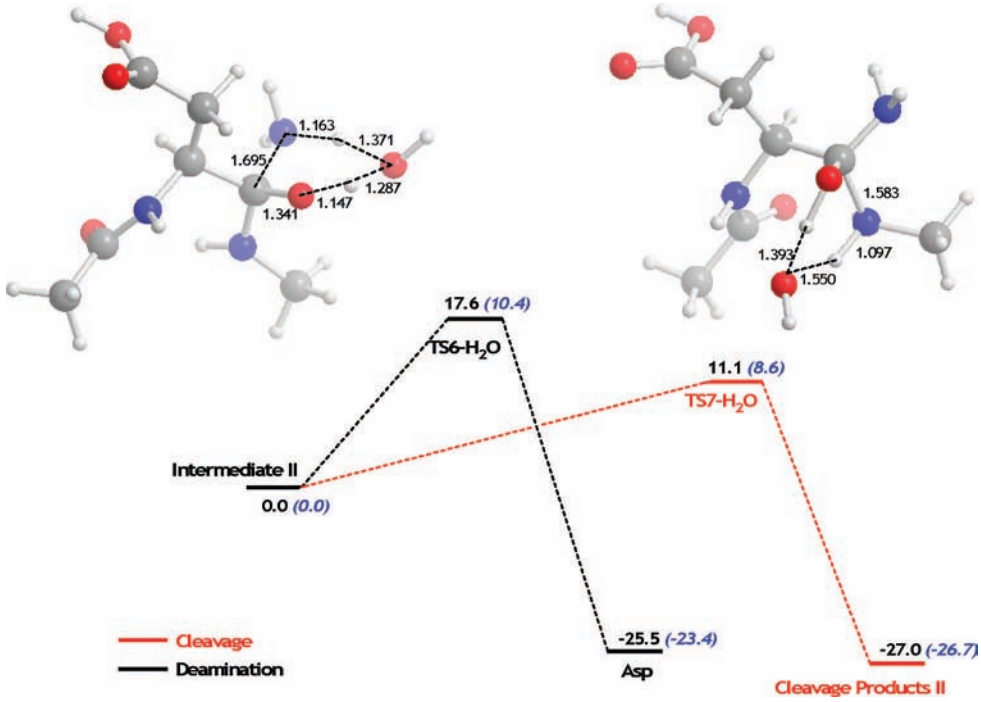

Figure 8. Relative free energies and optimized structures for transition states of the possible fates of intermediate II, one water-assisted.

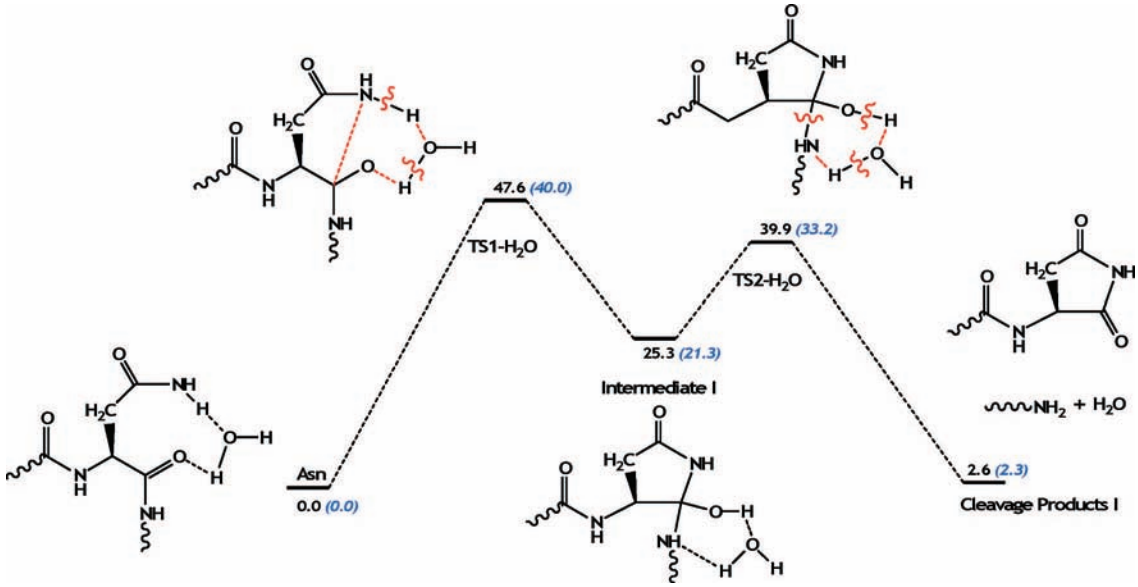

Figure 9. Relative free energies for peptide bond cleavage at Asn, water-assisted mechanism.

SCHEME 8: Peptide Bond Cleavage Mechanism for Asp Residues

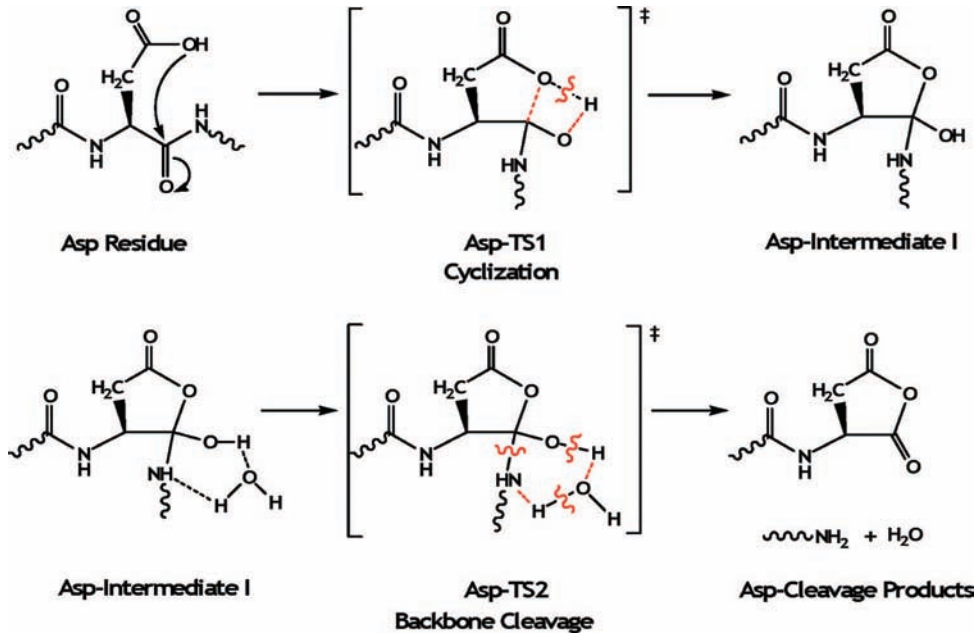

Backbone cleavage mechanisms for Asp and Asn reveal other similar features. The transition state structure for the nonassisted concerted cyclization mechanism (Asp-TS1, Figure 10) involves an asynchronous proton transfer accompanied by ring closure. In the water-assisted transition structure (Asp-TS1-H_2O, Figure 10) proton transfer via the water molecule takes place prior to actual ring closure. Water assistance has slightly decreased the energetics of this transition state.

Cyclization to Asp-intermediate I is followed by backbone cleavage (Scheme 8). The activation barrier for peptide fragmentation step is quite low (Figure 11), similar to the Asn case (Figure 4). Hydrolysis of Asp-intermediate I will not be discussed, because the outcome of such a reaction will be the starting structure itself.

The overall energetics of peptide bond cleavage at Asp is depicted in Figure 12. Although the activation barrier for the initial cyclization step is higher (30.5 kcal/mol) than the following cleavage step (16 kcal/mol), the latter is rate-determining in contrast with the Asn case.

Analysis of the energetics of backbone fragmentation at Asp residues might shed light on whether fragmentation is more likely to occur subsequent to deamidation of Asn into Asp, rather than cleavage at Asn itself. It is important to emphasize the difference in activation barriers (taken roughly as the relative free energy of the highest TS) of Asn (47.6 kcal/mol, Figure 9) and Asp (38.0 kcal/mol, Figure 12) cleavage. Peptide bond cleavage is energetically much more favorable for Asp. From the energetic data acquired in this study and previous computational studies done on deamidation of Asn,[21,22] it is therefore reasonable to suggest that in relatively flexible peptides, backbone cleavage at Asn residues may be preceded by deamidation into an Asp.

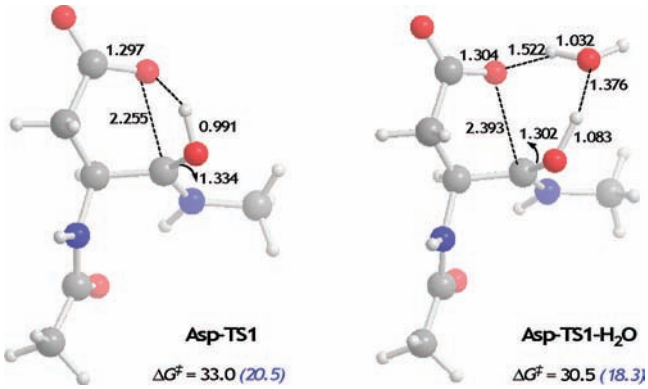

Figure 10. Optimized geometries and free energies of activation for the transition state of side-chain −OH attack on backbone Asp carbonyl, concerted waterless (Asp-TS1) and concerted one water-assisted (Asp-TS1-H_2O) mechanisms, respectively.

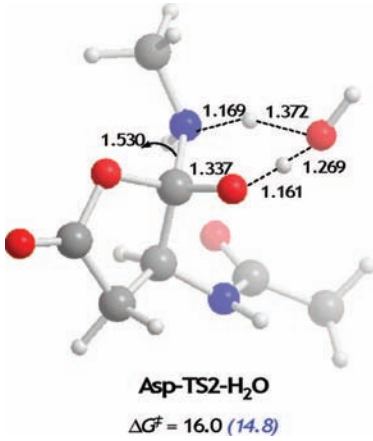

Figure 11. Optimized geometry and free energy of activation for transition state of backbone cleavage at Asp-intermediate I, concerted one water-assisted (Asp-TS2-H_2O) mechanisms.

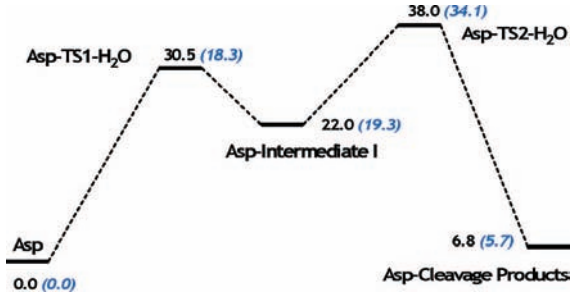

Figure 12. Relative free energies for peptide bond cleavage at Asp, water-assisted mechanism.

Conclusion

In this study, mechanisms leading to nonenzymatic peptide bond cleavage at Asn and Asp have been investigated using computational methods. Mechanism and energetics of peptide fragmentation at Asn have been comparatively analyzed with previous calculations on deamidation of Asn.[21] The cyclization step was shown to be the rate-determining step for backbone cleavage at Asn (Figure 9).

Although concerted cyclization for deamidation and cleavage have comparable activation barriers, previous computational studies have shown that deamidation does not necessarily involve such a reaction step. Direct hydrolysis of the Asn side chain[22] and cyclic imide formation via a tautomerization route[21] have lower activation barriers. Both of these processes are water assisted and therefore require the presence of water molecules. Backbone cleavage is unlikely to be competitive with deamidation in peptides with access to solvent molecules.

An important conclusion of this study is the energetics of backbone cleavage at Asp residues. The peptide fragmentation barrier is indeed much lower (approximately 10 kcal/mol) for Asp than for Asn. We therefore suggest that cleavage at Asn residues takes place after an Asn residue has deamidated into an Asp. Because the cleavage products differ for Asn (Scheme 4) and Asp (Scheme 8), experimental verification of this proposal appears to be quite feasible.

When deamidation is prevented by protein three-dimensional structure, due to hindrance of backbone rotation caused by sterics, secondary structure, and/or spatial distribution of neighboring residues, backbone cleavage of the Asn residue may ensue as a competitive reaction.

Acknowledgment. Computational resources provided by CINES (Centre Informatique National de l'Enseignement Supérieur) and TÜBİTAK ULAKBİM High Performance Computing Center. S.C. acknowledges a TÜBİTAK Ph.D. scholarship and a "co-tutelle" grant from the French Embassy in Ankara, Turkey. This research was supported by PIA-BOSPHORUS (Project PIA-TBAG-U/147 (105T275)) and BAP (Project 05HB501). We acknowledge the sixth framework project COSBIOM (FP6-2004-ACC-SSA-2, Project 517991) for travel and accommodation support. This research was supported in part by TÜBİTAK through TR-Grid e-Infrastructure Project. TR-Grid systems are hosted by TÜBİTAK ULAKBİM, Middle East Technical University, Pamukkale University, Çukurova University, Erciyes University, Boğaziçi University, and Istanbul Technical University of Turkey. Visit http://www.grid.org.tr for more information.

Supporting Information Available: Cartesian coordinates, energies, and imaginary frequencies for all optimized transition structures. This information is available free of charge via the Internet at http://pubs.acs.org.

References and Notes

(1) Robinson, A. B.; Rudd, C. *Curr. Top. Cell Regul.* **1974**, *8*, 247–295.
(2) Robinson, A. B.; Scothler, J. W.; McKerrow, J. H. *J. Am. Chem. Soc.* **1973**, *95*, 8156–8159.
(3) Bornstein, P.; Balian, G. *J. Biol. Chem.* **1970**, *245*, 4854–4856.
(4) Geiger, T.; Clarke, S. *J. Biol. Chem.* **1987**, *262*, 785–794.
(5) Voorter, C. E. M.; Haard-Hoekman, W. A.; Oetelaar, P. J. M.; Bloemendal, H.; Jong, W. W. *J. Biol. Chem.* **1988**, *263*, 19020–19023.
(6) Klotz, A. V.; Thomas, B. A. *J. Org. Chem.* **1993**, *58*, 6985–6989.
(7) Meinwald, C. Y.; Stimson, E. R.; Scheraga, H. A. *Int. J. Pept. Protein Res.* **1986**, *28*, 79–84.
(8) Capasso, S.; Mazzarella, L.; Sica, F.; Zagari, A.; Salvadori, S. *J. Chem. Soc., Perkin Trans. 2* **1993**, 679–682.
(9) Capasso, S.; Mazzarella, L.; Sica, F.; Zagon, A. *J. Pept. Res.* **1989**, *2*, 195–197.
(10) Capasso, S.; Salvadori, S. *J. Pept. Res.* **1999**, *54*, 377–382.
(11) Tam, J. P.; Riemen, M. W.; Merrifield, R. B. *Pept. Res.* **1988**, *1*, 6–18.
(12) Robinson, N. E.; Robinson, A. B. *J. Pept. Res.* **2004**, *63*, 437–448.
(13) Robinson, N. E.; Robinson, Z. W.; Robinson, B. R.; Robinson, A. L.; Robinson, M. R.; Robinson, A. B. *J. Pept. Res.* **2004**, *63*, 426–436.
(14) Robinson, N. E.; Robinson, A. B. *Molecular Clocks: Deamidation of Asparaginyl and Glutaminyl Residues in Peptides and Proteins*; Althouse Press: Cave Junction, OR, 2004.
(15) Konuklar, F. A.; Aviyente, V.; Sen, T. Z.; Bahar, I. *J. Mol. Model.* **2001**, *7*, 147–160.
(16) Konuklar, F. A.; Aviyente, V. *Org. Biomol. Chem.* **2003**, *1*, 2290–2297.
(17) Konuklar, F. A.; Aviyente, V.; Ruiz-Lopez, M. F. *J. Phys. Chem. A* **2002**, *106*, 11205–11214.

(18) Radkiewicz, J. L.; Zipse, H.; Clarke, S.; Houk, K. N. *J. Am. Chem. Soc.* **1996**, *118*, 9148–9155.
(19) Radkiewicz, J. L.; Zipse, H.; Clarke, S.; Houk, K. N. *J. Am. Chem. Soc.* **2001**, *123*, 3499–3506.
(20) Peters, B.; Trout, B. L. *Biochemistry* **2006**, *45*, 5384–5392.
(21) Catak, S.; Monard, G.; Aviyente, V.; Ruiz-López, M. F. *J. Phys. Chem. A* **2006**, *110*, 8354–8365.
(22) Catak, S.; Monard, G.; Aviyente, V.; Ruiz-López, M. F. In preparation.
(23) Capasso, S.; Mazzarella, L.; Sorrentino, G.; Balboni, G.; Kirby, A. J. *Peptides* **1996**, *17*, 1075–1077.
(24) Capasso, S.; Mazzarella, L.; Kirby, A.; Salvadori, S. *Pept. Sci.* **1998**, *40*, 543–551.
(25) Landon, M. *Methods Enzymol.* **1977**, *47*, 145–147.
(26) Piszkiewicz, D.; Landon, M.; Smith, E. L. *Biochem. Biophys. Res. Commun.* **1970**, *40*, 1173–1178.
(27) Kwong, M. Y.; Harris, R. J. *Protein Sci.* **1994**, *3*, 147–149.
(28) Tarelli, E.; Corran, P. H. *J. Pept. Res.* **2003**, *62*, 245–251.
(29) Joshi, A. B.; Kirsch, L. E. *Int. J. Pharm.* **2004**, *273*, 213–219.
(30) Joshi, A. B.; Rus, E.; Kirsch, L. E. *Int. J. Pharm.* **2000**, *203*, 115–125.
(31) Herrmann, K. A.; Wysocki, V. H. *J. Am. Soc. Mass Spectrom.* **2005**, *16*, 1067–1080.
(32) Joshi, A. B.; Sawai, M.; Kearney, W. R.; Kirsch, L. E. *J. Pharm. Sci.* **2005**, *94*, 1912–1927.
(33) Rozman, M. *J. Am. Soc. Mass Spectrom.* **2007**, *18*, 121–127.
(34) Gerschler, J. J.; Wier, K. A.; Hansen, D. E. *J. Org. Chem.* **2007**, *72*, 654–657.
(35) Stewart, J. J. P. *J. Comput. Chem.* **1989**, *10*, 221–264.
(36) Parr, R. G.; Yang, W. *Density-Functional Theory of Atoms and Molecules*; Oxford University Press: Oxford, U.K., 1989.
(37) Hohenberg, P.; Kohn, W. *Phys. Rev. B* **1964**, *136*, 864.
(38) Kohn, W.; Sham, L. *J. Phys. Rev. A* **1965**, *140*, 1133.
(39) Becke, A. D. *J. Chem. Phys.* **1993**, *98*, 5648–5652.
(40) Lee, C.; Yang, W.; Parr, R. G. *Phys. Rev. B* **1988**, *37*, 785.
(41) Madura, J.; Jorgensen, W. L. *J. Am. Chem. Soc.* **1986**, *108*, 2517–2527.
(42) Gonzalez, C.; Schlegel, H. B. *J. Chem. Phys.* **1989**, *90*, 2154–2161.
(43) Gonzalez, C.; Schlegel, H. B. *J. Phys. Chem.* **1990**, *94*, 5523–5527.
(44) Tomasi, J.; Mennucci, B.; Cancès, E. *J. Mol. Struct. (THEOCHEM)* **1999**, *464*, 211–226.
(45) Cancès, E. T.; Mennucci, B.; Tomasi, J. *J. Chem. Phys.* **1997**, *107*, 3032–3041.
(46) Mennucci, B.; Tomasi, J. *J. Chem. Phys.* **1997**, *106*, 5151–5158.
(47) Mennucci, B.; Cancès, E.; Tomasi, J. *J. Phys. Chem. B* **1997**, *101*, 10506–10517.
(48) Bondi, A. *J. Phys. Chem.* **1964**, *68*, 441–451.
(49) *Gaussian 03, Revision B.05*, Frisch, M. J. et al. Gaussian, Inc.: Wallingford, CT, 2004.
(50) Gorb, L.; Asensio, A.; Tunon, I.; Ruiz-Lopez, M. F. *Chem. Eur. J.* **2005**, *11*, 6743–6753.
(51) Robinson, N. E.; Robinson, A. B. *Proc. Natl. Acad. Sci. U.S.A.* **2001**, *98*, 4367–4372.
(52) Pries, F.; Kingma, J.; Janssen, D. B. *FEBS Lett.* **1995**, *358*, 171–174.

JP8015497